Modeling the Highly Effective Object for Continuous Compaction Control of the Cyber-Physical Road-Construction System

Andrey Prokopev, Zhasurbek Nabizhanov, Rurik Emelyanov, and Vladimir Ivanchura

Abstract Compaction of hot mix asphalt (HMA) is one of the most important processes in the construction of road surfaces. The technologies of continuous compaction control (CCC) and intelligent compaction (IC) are based on algorithmic and software–technical means for processing informative signals and presenting the results of determining material compaction indicators. One of the possible reserves for increasing the efficiency of compaction is an increase in the compaction coefficient by the working bodies of stackers. The most effective management of road construction in real-time is carried out when asphalt pavers and road rollers interact as part of the existing cyber-physical system. In this chapter, using the state space method, a mathematical model of the HMA compaction process with a highly efficient stacker working body as an object of continuous nondestructive compaction control is obtained. The use of the state space method provided a clear formalization and automation of computational procedures, increasing the efficiency of theoretical research of the object using modern software. The model takes into account the design elements of the working body and the properties of the compacted material. The output parameters of the object model are intended for process dynamics analysis, continuous compaction monitoring, measurement, and control automation. The chapter presents a computer model of the object in the MATLAB/Simulink and the results of a computational experiment to model the workflow of the research object. The development of cyber-physical systems helps to increase the efficiency of managing sets of automated compacting machines at a construction site.

A. Prokopev (✉) · Z. Nabizhanov · R. Emelyanov · V. Ivanchura
Siberian Federal University, 79 Svobodny, Krasnoyarsk 660041, Russia
e-mail: prok1@yandex.ru

Z. Nabizhanov
e-mail: jasur150691@yandex.ru

R. Emelyanov
e-mail: ert-44@yandex.ru

V. Ivanchura
e-mail: ivan43ura@yandex.ru

A. G. Kravets et al. (eds.), *Cyber-Physical Systems: Modelling and Intelligent Control*, Studies in Systems, Decision and Control 338,
https://doi.org/10.1007/978-3-030-66077-2_14

Keywords Cyber-physical system · Paver · Highly effective working body · Dynamic model · State-space · Continuous compaction control

1 Introduction

Changes of requirements for asphalt pavement quality create conditions for the implementation of intelligent and "smart" technologies in the road building industry. The main stages of the asphalt pavements construction process affect coating performance [1]: manufacture, transportation from the plant to the facility, spreading, mixture placing, and compaction. Mixture compaction by pavers and road rollers eliminates up to 50% of the disadvantages of asphalt pavements and increases their service life [2].

Systems of continuous non-destructive compaction control of hot mix asphalt with intelligent compaction technologies, continuous compaction control [3–9], installed on vibratory rollers, and a neural network automatic control system [10, 11] are modern methods of compaction control of road surfaces.

Known methods and control means have a significant error, do not allow to evaluate the efficiency of the rolling process, and are not able to record the compaction characteristics [12]. These drawbacks are confirmed in many scientific papers [12–14].

Over the 40 years of the existence of the idea of continuous compaction control, the developers of automatic systems have not come up with effective means of reducing drawbacks in measuring the compaction degree of hot mix asphalt. The main variable of control systems is the acceleration of the vibratory roller. However, the material characteristics during compaction are not constant. The structure of the road-building mixture, humidity, temperature of the layer, stiffness of the base, layer thickness are changing. In well-known developments of continuous compaction control systems of leading companies such as Trimble, MOBA, Topcon, Hydac, etc., there are no data on the consideration of several significant factors in predicting the compaction effectiveness. Thus, the problem of increasing the efficiency of continuous non-destructive compaction control, taking into account significant factors of the changing properties of the material, strain–stress state, requires a solution.

The relevance of solving this problem increases in connection with the development of the scientific field—cybernetic physics [15]. The automation level of road-building machines—objects of cyber-physical systems (CPS), should be high. The performance of the entire CPS depends on the quality of measurements and forecasts of the parameters of the automated control system. We can state the presence of developed mathematical models of the compaction process by vibratory rollers [3–20], and oscillating rollers, which allows solving current issues of non-destructive technologies in the road construction field.

The set of road construction machines providing compaction of hot mix asphalt, in addition to road rollers, includes pavers that can compact the material to standard values when equipped with a highly effective working body. Depending on the achieved compaction factor, we can reduce the number and types of road rollers, the number of passes after the stacker. These technological measures boost productivity and cost reduction of road construction. But it is impossible to completely exclude the use of existing road rollers with existing technologies isn't possible, because they are necessary to confirm the achieved compaction coefficient of the material and increase the structural strength of asphalt concrete. To increase the efficiency and productivity of the compaction processes of pavements, it is necessary to carry out continuous non-destructive compaction control and regulation of operating modes—tamping frequency, frequency of plate vibration, impulse movements frequency of the pressing bars, taking into account the technological capabilities of modern pavers. Currently, such automatic control and management systems for pavers are not available. Having such systems, it is possible to create a "smart" paver with a significant increase in productivity by optimizing the compaction process and reducing the workload of the driver. To increase the effectiveness of scientific research and the design of objects of cyber-physical systems, mathematical models of real processes are needed.

This work is devoted to the theoretical description of the object of continuous compaction control of a cyber-physical road-building system—an asphalt paver with a highly effective working body. Theoretical studies on the compaction of various materials (soils, asphalt mixtures) have been and are being carried out by many Russian [16] and foreign scientists [17–20]. The disadvantages of previously developed mathematical models are the problems of algorithmization of tasks, computational difficulties in the study of dynamic systems, the design of automatic control and management systems.

To eliminate these drawbacks and to increase the efficiency of theoretical research of the control object using the modern MATLAB/Simulink software, it is recommended to use the state space method, which allows making clear characterization and automation of computational procedures [21–23].

2 The Mathematical Formulation of the Problem

For research, a highly effective working body was taken in the following composition of the compacting units: tamper—vibration plate—two pressing bars. The compaction process of the mixture is carried out with constant contact of the vibrating plate with the mixture. The main compaction is performed by compressing the mixture with a horizontal platform of a tamping beam when moving in a vertical plane for 4–6 effects. A vibrating plate and pressing bars fix the achieved compaction result and improve the structure of the material. Pressing bars creates periodic impulse loadings with a frequency of 50–70 Hz and pressure in the hydraulic system from 5 to 15 MPa [24].

The dynamic parameters of compacting units and particles of material are frequency, amplitude, speed, and acceleration.

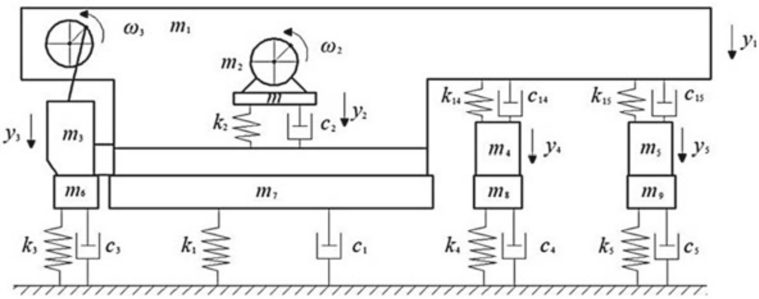

Fig. 1 The dynamic model of the mixture compaction process by the working body (tamper, vibration plate, two pressure bars) of the paver

A simulation model of a dynamic model of the compaction process of the mixture with a highly effective working body of the paver is obtained based on the technical documentation [24], Fig. 1.

On the Fig. 1 the following notation is used: m_1—mass of the smoothing plate frame, kg; m_2—weight of vibrator, kg; m_3—weight of tamper, kg; m_4—weight of the first pressure bar, kg; m_5—weight of the second pressure bar, kg; m_6—weight of the mix under the tamper, kg; m_7—weight of the mix under the vibration plate, kg; m_8—weight of mix under the first pressure bar, kg; m_9—weight of the mix under the second pressure bur, kg; k_1—coefficient of elastic resistance of the compacted mix under the plate, N/m; c_1—damping coefficient of the compacted mix under the plate, N s/m; k_2—coefficient of elastic resistance of the shock absorbers of the vibrator, N/m; c_2—damping coefficient of shock absorbers of the vibrator, N s/m; k_3—coefficient of elastic resistance of the compacted mix under the tamper, N/m; c_3—damping coefficient of the compacted mix under the tamper, N s/m; k_4—coefficient of elastic resistance of the compacted mix under the first pressure bar, N/m; k_5—coefficient of elastic resistance of the compacted mix under the second pressure bar, N/m; c_4—damping coefficient of the compacted mixture under the second pressure bar, N s/m; k_{14} and k_{15}—coefficient of elastic resistance of the first and second pressure bars, N/m; c_{14} and c_{15}—damping coefficient of the first and second pressure bars, N s/m; y_1, y_2, y_3, y_4 and y_5—the moving system elements, respectively, m.

We developed a mathematical model that presents both the vibration dynamics of structural elements and the rheological properties of the compacted material. Differential equations describing the movement of the first and second pressure bar

$$\begin{aligned}(m_4 + m_8) \cdot \ddot{y}_4 \quad &- c_{14} \cdot \dot{y}_1 + (c_4 + c_{14}) \cdot \dot{y}_4 - k_{14} \cdot y_1 \\ &+ (k_4 + k_{14}) \cdot y_4 = F_4 + m_4 \cdot g + m_8 \cdot g, \end{aligned} \tag{1}$$

$$\begin{aligned}(m_5 + m_9) \cdot \ddot{y}_5 \quad &- c_{15} \cdot \dot{y}_1 + (c_5 + c_{15}) \cdot \dot{y}_5 - k_{15} \cdot y_1 \\ &+ (k_5 + k_{15}) \cdot y_5 = F_5 + m_5 \cdot g + m_9 \cdot g, \end{aligned} \tag{2}$$

where F_4, F_5 is the force of the first and second pressure bar, respectively, N.

The differential equation of the smoothing plate vibrator

$$m_2 \cdot \ddot{y}_2 - c_2 \cdot \dot{y}_1 + c_2 \cdot \dot{y}_2 - k_2 \cdot y_1 + k_2 \cdot y_2 = m \cdot \omega_2^2 \cdot r \cdot \sin(\omega_2 \cdot t), \quad (3)$$

where F_3 is the force of tamping beam ram, N.

With allowance for the principle of relative motion, we obtain an additional equation

$$y_3 = y_1 + e \cdot \sin(\omega_3 \cdot t), \quad (4)$$

where e—tamper eccentricity size, m; ω_3—the rotational speed of the tamper gear, rad/s.

Substituting Eq. (4) into (3) with transformations, we obtain the following equation

$$\begin{aligned} F_3 = (m_3 + m_6) \cdot \ddot{y}_1 + c_3 \cdot \dot{y}_1 + k_3 \cdot y_1 - (m_3 + m_6) \cdot e \cdot \omega_3^2 \cdot \sin(\omega_3 \cdot t) \\ + k_3 \cdot e \cdot \sin(\omega_3 \cdot t) + c_3 \cdot e \cdot \omega_3 \cdot \sin(\omega_3 \cdot t + \pi/2) - m_6 \cdot g. \end{aligned} \quad (5)$$

The differential equation of smoothing plate motion

$$\begin{aligned} (m_1 + m_7) \cdot \ddot{y}_1 + (c_1 + c_2 + c_{14} + c_{15}) \cdot \dot{y}_1 - c_2 \cdot \dot{y}_2 - c_{14} \cdot \dot{y}_4 - c_{15} \cdot \dot{y}_5 \\ + (k_1 + k_2 + k_{14} + k_{15}) \cdot y_1 - k_2 \cdot y_2 - k_{14} \cdot y_4 - k_{15} \cdot y_5 \\ = -F_3 - F_4 - F_5 + (m_1 + m_7) \cdot g. \end{aligned} \quad (6)$$

Substituting Eq. (5) into (6), we obtain the following differential expression

$$\begin{aligned} (m_1 + m_7 + m_3 + m_6) \cdot \ddot{y}_1 + (c_1 + c_2 + c_3 + c_{14} + c_{15}) \cdot \dot{y}_1 - c_2 \cdot \dot{y}_2 - c_{14} \cdot \dot{y}_4 - c_{15} \cdot \dot{y}_5 \\ + (k_1 + k_2 + k_3 + k_{14} + k_{15}) \cdot y_1 - k_2 \cdot y_2 - k_{14} \cdot y_4 - k_{15} \cdot y_5 \\ = -F_4 - F_5 + \left([m_3 + m_6] \cdot e \cdot \omega_3^2 - k_3 \cdot e\right) \cdot \sin(\omega_3 \cdot t) \\ -c_3 \cdot e \cdot \omega_3 \cdot \sin(\omega_3 \cdot t + \pi/2) + (m_1 + m_6 + m_7) \cdot g. \end{aligned} \quad (7)$$

3 Methods and Materials

The state-space method allows you to represent the control system in the form of an equations system [21, 22]:

$$\dot{x}(t) = A(t) \cdot x(t) + B(t) \cdot u(t), \quad (8)$$

$$y(t) = C(t) \cdot x(t) + D(t) \cdot u(t), \tag{9}$$

where $x(t)$ is the state vector of dimension $(n \times 1)$, whose components are state variables of the n-th order system, $x(t) = [x_1(t),\ x_2(t), \ldots,\ x_n(t)]^T$, $y(t)$ is the dimension output vector $(p \times 1)$, whose components are the output variables of the system, $y(t) = \left[y_1(t),\ y_2(t), \ldots,\ y_p(t)\right]^T$, $u(t)$ is the dimension input vector $(r \times 1)$, whose components are the output variables of the system $u(t) = [u_1(t),\ u_2(t), \ldots,\ u_r(t)]^T$, $A(t)$ is the matrix of the system $(n \times n)$, $B(t)$ is the input matrix $(n \times m)$, $C(t)$ is the output matrix $(p \times n)$, $D(t)$ is the detour matrix $(p \times m)$, determining the direct dependence of the output on the input,p is the output quantity number.

The state parameters of a dynamic system are defined as follows: x_1 is the vertical movement of the vibrating plate, $x_1 = y_1$, x_2 is the vertical velocity of the vibrating plate, $x_2 = \dot{y}_1$, x_3 is the vibrator vertical movement, $x_3 = y_2$, x_4 is the vibrator vertical velocity $x_4 = \dot{y}_2$, x_5 is the first pressing bar vertical movement, $x_5 = y_4$, x_6 is the first pressing bar vertical velocity, $x_6 = \dot{y}_4$, x_7 is the second pressing bar vertical movement, $x_7 = y_5$, x_8 is the second pressing bar vertical velocity, $x_8 = \dot{y}_5$.

We get a mathematical formulation of the object dynamics in the form of Cauchy on the rearrangement of the equations system of (1)–(7):

$$\begin{aligned}
&x_2 = \dot{y}_1; \\
&\dot{x}_2 = \frac{\begin{bmatrix} -(c_1 + c_2 + c_3 + c_{14} + c_{15}) \cdot x_2 + c_2 \cdot x_4 + c_{14} \cdot x_6 + c_{15} \cdot x_8 \\ +(k_1 + k_2 + k_3 + k_{14} + k_{15}) \cdot x_1 + k_2 \cdot x_3 + k_{14} \cdot x_5 + k_{15} \cdot x_7 - F_4 - F_5 \\ +\left(\left[m_3 + m_6\right] \cdot e \cdot \omega_3^2 - k_3 \cdot e\right) \cdot \sin(\omega_3 \cdot t) \\ + c_3 \cdot e \cdot \omega_3 \cdot \sin(\omega_3 \cdot t + \pi/2) + (m_1 + m_6 + m_7) \cdot g \end{bmatrix}}{m_1 + m_3 + m_6 + m_7}, \\
&x_4 = \dot{y}_2;\ \dot{x}_4 = \frac{1}{m_2} \cdot \left(c_2 \cdot x_2 - c_2 \cdot x_4 + k_2 \cdot x_1 - k_2 \cdot x_3 + m \cdot r \cdot \omega_2^2 \cdot \sin(\omega_2 \cdot t)\right), \\
&x_6 = \dot{y}_4;\ \dot{x}_6 = \frac{1}{m_4 + m_8} \cdot \left(c_{14} \cdot x_2 - \left[c_4 + c_{14}\right] \cdot x_6 + k_{14} \cdot x_1 - \left[k_4 + k_{14}\right] \cdot x_5 + F_4 + \left[m_4 + m_8\right] \cdot g\right), \\
&x_8 = \dot{y}_5;\ \dot{x}_8 = \frac{1}{m_5 + m_9} \cdot \left(c_{15} \cdot x_2 - \left[c_5 + c_{15}\right] \cdot x_8 + k_{15} \cdot x_1 - \left[k_5 + k_{15}\right] \cdot x_7 + F_5 + \left[m_5 + m_9\right] \cdot g\right).
\end{aligned}$$

We can obtain the following results by moving these parameters into the corresponding vector and matrix.

Enter parameter value

$$\begin{aligned}
M &= m_1 + m_3 + m_6 + m_7\,, \\
K &= k_1 + k_2 + k_3 + k_{14} + k_{15}\,, \\
Q &= c_1 + c_2 + c_3 + c_{14} + c_{15}\,.
\end{aligned}$$

Then the model of the process understudy in the state space, in the vector–matrix form

$$y(t) = C \cdot x(t) + D \cdot u(t)\,,$$

$$\begin{bmatrix} y_1(t)\\ y_2(t)\\ y_3(t)\\ y_4(t)\\ y_5(t)\\ y_6(t)\\ y_7(t)\\ y_8(t) \end{bmatrix} = \begin{bmatrix} 1&0&0&0&0&0&0&0\\ 0&1&0&0&0&0&0&0\\ 0&0&1&0&0&0&0&0\\ 0&0&0&1&0&0&0&0\\ 0&0&0&0&1&0&0&0\\ 0&0&0&0&0&1&0&0\\ 0&0&0&0&0&0&1&0\\ 0&0&0&0&0&0&0&1 \end{bmatrix} \cdot \begin{bmatrix} x_1(t)\\ x_2(t)\\ x_3(t)\\ x_4(t)\\ x_5(t)\\ x_6(t)\\ x_7(t)\\ x_8(t) \end{bmatrix} + \begin{bmatrix} 0&0&0&0\\ 0&0&0&0\\ 0&0&0&0\\ 0&0&0&0\\ 0&0&0&0\\ 0&0&0&0\\ 0&0&0&0\\ 0&0&0&0 \end{bmatrix} \cdot u(t)\,,$$

$$\dot{x}(t) = A \cdot x(t) + B \cdot u(t)\,,$$

$$\begin{bmatrix} \dot{x}_1(t)\\ \dot{x}_2(t)\\ \dot{x}_3(t)\\ \dot{x}_4(t)\\ \dot{x}_5(t)\\ \dot{x}_6(t)\\ \dot{x}_7(t)\\ \dot{x}_8(t) \end{bmatrix} = \begin{bmatrix} 0 & 1 & 0 & 0 & 0 & 0 & 0 & 0\\ -\frac{K}{M} & -\frac{Q}{M} & \frac{k_2}{M} & \frac{c_2}{M} & \frac{k_{14}}{M} & \frac{c_{14}}{M} & \frac{k_{15}}{M} & \frac{c_{15}}{M}\\ 0 & 0 & 0 & 1 & 0 & 0 & 0 & 0\\ \frac{k_2}{m_2} & \frac{c_2}{m_2} & -\frac{k_2}{m_2} & -\frac{c_2}{m_2} & 0 & 0 & 0 & 0\\ 0 & 0 & 0 & 0 & 0 & 1 & 0 & 0\\ \frac{k_{14}}{m_4+m_8} & \frac{c_{14}}{m_4+m_8} & 0 & 0 & -\frac{k_4+k_{14}}{m_4+m_8} & -\frac{c_4+c_{14}}{m_4+m_8} & 0 & 0\\ 0 & 0 & 0 & 0 & 0 & 0 & 0 & 1\\ \frac{k_{15}}{m_5+m_9} & \frac{c_{15}}{m_5+m_9} & 0 & 0 & 0 & 0 & -\frac{k_5+k_{15}}{m_5+m_9} & -\frac{c_5+c_{15}}{m_5+m_9} \end{bmatrix}$$

$$\cdot \begin{bmatrix} x_1(t)\\ x_2(t)\\ x_3(t)\\ x_4(t)\\ x_5(t)\\ x_6(t)\\ x_7(t)\\ x_8(t) \end{bmatrix} + \begin{bmatrix} 0 & 0 & 0 & 0\\ \frac{1}{M} & 0 & 0 & 0\\ 0 & 0 & 0 & 0\\ 0 & \frac{1}{m_2} & 0 & 0\\ 0 & 0 & 0 & 0\\ 0 & 0 & \frac{1}{m_4+m_8} & 0\\ 0 & 0 & 0 & 0\\ 0 & 0 & 0 & \frac{1}{m_5+m_9} \end{bmatrix} \cdot u(t)\ ,$$

where

$$u(t) = \begin{bmatrix} -F_4 - F_5 + \left([m_3 + m_6] \cdot e \cdot \omega_3^2 - k_3 \cdot e\right) \cdot \sin(\omega_3 \cdot t)\\ -c_3 \cdot e \cdot \omega_3 \cdot \sin(\omega_3 \cdot t + \pi/2) + (m_1 + m_6 + m_7) \cdot g\\ m \cdot \omega_2^2 \cdot r \cdot \sin(\omega_2 \cdot t)\\ F_4 + (m_4 + m_8) \cdot g\\ F_5 + (m_5 + m_9) \cdot g \end{bmatrix}.$$

4 Results and Analysis

A simulation model is obtained in the environment of the MATLAB/Simulink program. The initial data from scientific work [25] were used to simulate the process.

$$k_1 = 4.2 \cdot 10^6 \text{ N/m}, \; k_2 = 10.3 \cdot 10^7 \text{ N/m}, \; k_3 = 1.68 \cdot 10^6 \text{ N/m},$$
$$k_4 = 4.2 \cdot 10^6 \text{ N/m}, k_5 = 5 \cdot 10^6 \text{ N/m}, \; k_{14} = 1.1 \cdot 10^4 \text{ N/m},$$
$$k_{15} = 1.1 \cdot 10^4 \text{ N/m}, \; c_1 = 1200 \text{ N} \cdot \text{s/m}, \; c_2 = 17600 \text{ N} \cdot \text{s/m},$$
$$c_3 = 3160 \text{ N} \cdot \text{s/m}, c_4 = 1200 \text{ N} \cdot \text{s/m}, c_5 = 1200 \text{ N} \cdot \text{s/m},$$
$$c_{14} = 200 \text{ N} \cdot \text{s/m}, c_{15} = 200 \text{ N} \cdot \text{s/m},$$
$$m = 9.6 \text{ kg}, m_1 = 3000 \text{ kg}, m_2 = 80 \text{ kg}, \; m_3 = 260 \text{ kg}, \; m_4 = 260 \text{ kg},$$
$$m_5 = 260 \text{ kg}, m_6 = 0.2 \cdot m_3, \; m_7 = 0.2 \cdot m_1, \; m_8 = 0.2 \cdot m_4,$$
$$m_9 = 0.2 \cdot m_5, r = 0,035 \text{ m}, e = 0,007 \text{ m}, \; f_2 = 20 \text{ Hz}, \; f_3 = 15 \text{ Hz},$$
$$f_4 = 25 \text{ Hz} \; f_5 = 25 \text{ Hz}, \; F_4 = 9000 \text{ N}, F_5 = 9000 \text{ N}.$$

A simulation model of the studied process is presented in Fig. 2.

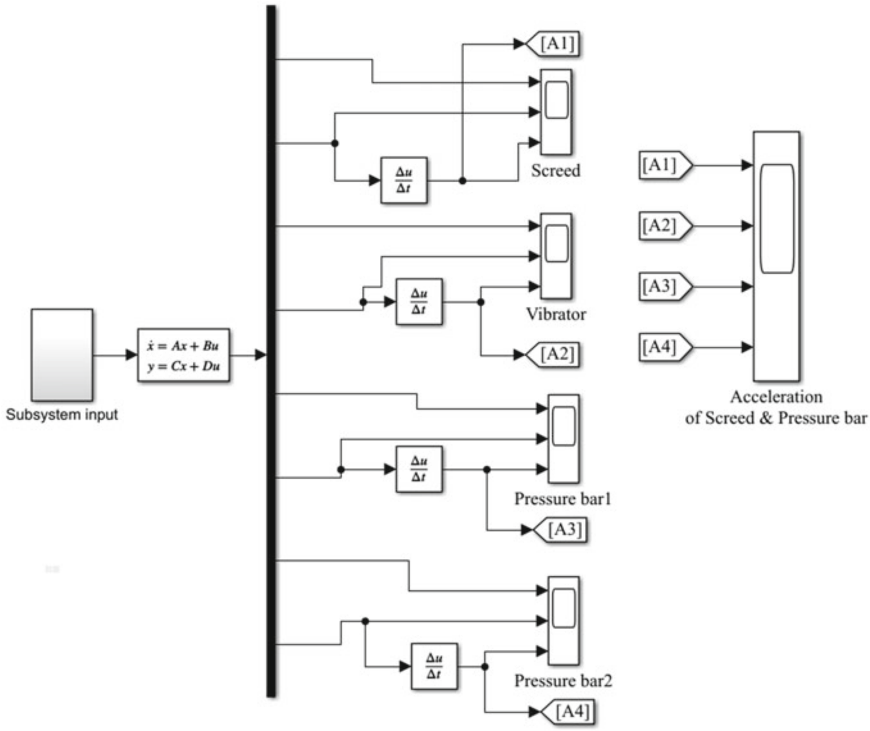

Fig. 2 Simulation model in the language of the program MATLAB/Simulink

The timing diagram of work process parameters was obtained by computer simulation: displacement, velocity, acceleration. Figure 3 shows the graphical dependencies for the vibration plate.

The obtained dependencies correspond to the oscillatory process, and stability features of a dynamic system are observed. The vibration plate acceleration with peak values up to 25 m/s^2 indicates a good correlation with the research results [1, 25].

The simulation results of the compaction process of the material by the second pressing bar are shown in Fig. 4.

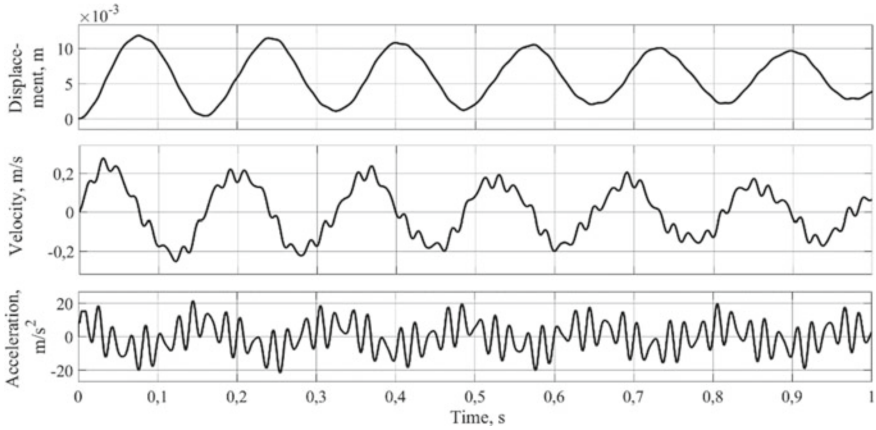

Fig. 3 The dependences of the oscillatory process parameters of the smoothing plate of the paver

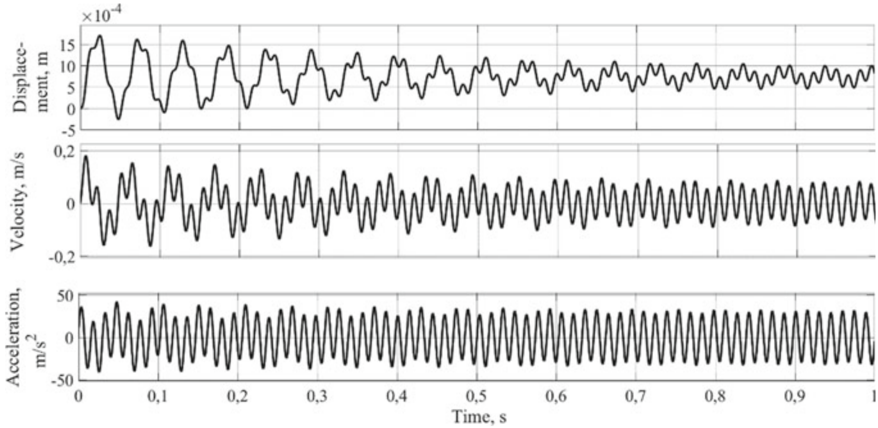

Fig. 4 The dependences of the oscillatory process parameters of the second pressing bar of the paver working body

The graphs in Fig. 4 show a significant decrease in the amount of the bar movement, a slight increase in acceleration due to gear vibration. Dependencies correspond to the nature of the physics of the workflow.

5 Determination of the Transfer Function of the Control Object

The transfer function was determined to conduct a study of a mathematical model using block simulation software. As a result of the MATLAB program tools implementation, we obtained advanced functions with the regulated variable—the angular frequency of vibration.

Transfer function regulated variable—vibrating plate displacement

$$W(s) = \frac{\begin{bmatrix} 0,0002556 \cdot s^6 + 0,05853 \cdot s^5 + 338,2 \cdot s^4 + 4890 \cdot s^3 \\ +1,119 \cdot 10^7 \cdot s^2 + 6,576 \cdot 10^7 \cdot s + 9,337 \cdot 10^{10} \end{bmatrix}}{\begin{bmatrix} s^8 + 234,7 \cdot s^7 + 1,351 \cdot 10^6 \cdot s^6 + 2,147 \cdot 10^7 \cdot s^5 + 4,667 \cdot 10^{10} \cdot s^4 \\ +3,446 \cdot 10^{11} \cdot s^3 + 4,391 \cdot 10^{14} \cdot s^2 + 8,324 \cdot 10^{14} \cdot s + 5,51 \cdot 10^{17} \end{bmatrix}},$$

transfer function regulated variable—vibrating plate velocity

$$W(s) = \frac{\begin{bmatrix} 0,0002556 \cdot s^7 + 0,05853 \cdot s^6 + 338,2 \cdot s^5 + 4890 \cdot s^4 \\ +1,119 \cdot 10^7 \cdot s^3 + 6,576 \cdot 10^7 \cdot s^2 + 9,337 \cdot 10^{10} \cdot s \end{bmatrix}}{\begin{bmatrix} s^8 + 234,7 \cdot s^7 + 1,351 \cdot 10^6 \cdot s^6 + 2,147 \cdot 10^7 \cdot s^5 + 4,667 \cdot 10^{10} \cdot s^4 \\ +3,446 \cdot 10^{11} \cdot s^3 + 4,391 \cdot 10^{14} \cdot s^2 + 8,324 \cdot 10^{14} \cdot s + 5,51 \cdot 10^{17} \end{bmatrix}}.$$

The obtained transfer functions correspond to the correct form since the degree of the numerator is less than the degree of the denominator. In further studies, when designing an automatic controller, it is necessary to take into account the high order of the mathematical model of the control object.

6 Conclusion

The chapter discusses the task of simulation as a highly efficient object of continuous compaction control of the cyber-physical system. A mathematical model of the mixture compaction process is obtained by a highly effective working body of the paver using the state space method. The obtained model was verified by simulation in the environment of the MATLAB/Simulink program. The results of the work are a stage of scientific research in the field of designing intelligent control and management systems for cyber-physical road-building systems.

Acknowledgements The reported study was funded by the RFBR project No. 19-37-90052.

References

1. Sun, J., Xu, G.: Dynamics modeling and analysis of paver screed based on computer simulation. J. Appl. Sci. **13**, 1059–1065 (2013). https://doi.org/10.3923/jas.2013.1059.1065
2. Prokopyev, A.P., Ivanchura, V.I., Emelianov, R.T., Palchikov, P.A.: Implementation of the concept of automation and intellectualization of management of road construction processes. Vestnik MGSU, **13**, **1**(112), 61–70 (2018). https://doi.org/10.22227/1997-0935.2018.1.61-70
3. Xu, Q., Chang, G.K.: Adaptive quality control and acceptance of pavement material density for intelligent road construction. Automat. Constr. **62**, 78–88 (2015). https://doi.org/10.1016/j.autcon.2015.11.004
4. Anderegg, R., Kaufmann, K.: Intelligent compaction with vibratory rollers: feedback control systems in automatic compaction and compaction control. Transp. Res. Board. **1868**, 124–134 (2004). https://doi.org/10.3141/1868-13
5. Hu, W., Shu, X., Huang, B., Woods, M.: Field investigation of intelligent compaction for hot mix asphalt resurfacing. Front. Struct. Civil Eng. **11**(1), 47–55 (2017). https://doi.org/10.1007/s11709-016-0362-x
6. Fang, X., Bian, Y., Yang, M., Liu, G.: Development of a path following control model for an unmanned vibratory roller in vibration compaction. Adv. Mech. Eng. **10**(5), 1–16 (2018). https://doi.org/10.1177/1687814018773660
7. Bian, Y., Fang, X., Yang, M., Zhao, Z.: Automatic rolling control for unmanned vibratory roller based on fuzzy algorithm. J. Tongji Univ. (Natural Science) **45**(12), 1831–1838 (2017). https://doi.org/10.11908/j.issn.0253-374x.2017.12.013
8. Zhu, S., Li, X., Wang, H., Yu, D.: Development of an automated remote asphalt paving quality control system. Transp. Res. Rec. **2672**(26), 28–39 (2018). https://doi.org/10.1177/0361198118758690
9. Liu, D.H., Li, Z.L., Lian, Z.H.: Compaction quality assessment of earth-rock dam materials using rollerintegrated compaction monitoring technology. Automat. Constr. **44**, 234–246 (2014). https://doi.org/10.1016/j.autcon.2014.04.016
10. Barman, M., Nazari, M., Imran, S.A., Commuri, S., Zaman, M., Beainy, F., Singh, D.: Quality control of subgrade soil using intelligent compaction. Innov. Infrastruct. Sol. **1**(1), 23 (2016). https://doi.org/10.1007/s41062-016-0020-0
11. Barman, M., Imran, S.A., Nazari, M., Commuri, S., Zaman, M.: Use of intelligent compaction in detecting and remediating under-compacted spots during compaction of asphalt layers. In: Hossain, Z., Zhang, J., Chen, C. (eds.) Solving Pavement and Construction Materials Problems with Innovative and Cutting-edge Technologies. GeoChina 2018. Sustainable Civil Infrastructures. Springer, Cham, pp. 131–141 (2019). https://doi.org/10.1007/978-3-319-95792-0_11
12. Zakharenko, A.V., Permyakov, V.B., Molokova, L.V.: Road rollers: theory, calculation, application: monograph. SPb.: LAN Publishing House, 328 p. (2018) ISBN 978-5-8114-3201-1
13. Hua, T., Yang, X., Yao, Q., Li, H.: Assessment of real-time compaction quality test indexes for rockfill material based on roller vibratory acceleration analysis. Adv. Mater. Sci. Eng. **2018**, 1–15 (2018). https://doi.org/10.1155/2018/2879321
14. Liu, D., Gao, L.: Analysis and improvement of roller vibration behavior-based indexes for monitoring compaction quality of earth-rock dams. J. Hydroelectr. Eng. **37**(4), 111–120 (2018).https://doi.org/10.11660/slfdxb.20180411
15. Fradkov, A.L.: Horizons of cybernetical physics. Philos. Trans. Math. Phys. Eng. Sci. **375**(2088), 20160223 (2017). https://doi.org/10.1098/rsta.2016.0223

16. Miheyev, V.V., Saveliev, S.V.: Modelling of deformation process for the layer of elastoviscoplastic media under surface action of periodic force of arbitrary type. J. Phys. Conf. Ser. **944**(1), 012079 (2018). https://doi.org/10.1088/1742-6596/944/1/012079
17. Rinehart, R.V., Mooney, M.A.: Instrumentation of a roller compactor to monitor vibration behavior during earthwork compaction. Autom. Constr. **17**, 144–150 (2008)
18. Beainy, F., Commuri, S., Zaman, M.: Dynamical response of vibratory rollers during the compaction of asphalt pavements. J. Eng. Mech. **140**(7), 04014039 (2014). https://doi.org/10.1061/(asce)em.1943-7889.0000730
19. Imran, S.A., Commuri, S., Barman, M., Zaman, M., Beainy, F.: Modeling the dynamics of asphalt-roller interaction during compaction. J. Constr. Eng. And Manag. **143**(7), 1763–1770 (2017). https://doi.org/10.1061/(ASCE)CO.1943-7862.0001293
20. Wang, J., Sha, A., Hu, L.: Modelling vibratory roller-soil system dynamics using discrete element method. Int. J. Eng. Model. **31**(3), 35–50 (2019). https://doi.org/10.31534/engmod.2018.3.ri.03m
21. Derusso, P.M., Roy, R.J., Close, C.M.: State variables for engineers (1965). Wiley, New York, 608 p.
22. Phillips, Ch.L., Harbor, R.D.: Feedback Control Systems (2010). Pearson, 784 p.
23. Prokopev, A.P., Nabizhanov, Zh.I., Ivanchura, V.I., Emelyanov, R.T.: Modeling the nondestructive control of road surfaces compaction. J. Phys. Conf. Ser. **1399**, 044094 (2019). https://doi.org/10.1088/1742-6596/1399/4/044094
24. WIRTGEN GROUP Concentrating on the essentials: high quality paving RoadNews. **7**, 28–47 (2019). https://media.voegele.info/media/03_voegele/aktuelles_und_presse/roadnews_magazin/roadnews_07/RadNews_07__en.pdf
25. Liu, G., Tian, J., Xiao, Z., Xu, L., Yu, Y.: Simulation of dynamic character of compacting mechanism of paver. J. Agric. Mach. **36**(11), 34–37 (2005)